Cathodoluminescence study of dislocation-related luminescence from small-angle grain boundaries in multicrystalline silicon

Woong Lee,[1,2] Jun Chen,[1] Bin Chen,[1,3] Jiho Chang,[2] and Takashi Sekiguchi[1,3,a)]
[1]*Advanced Electronic Materials Center, National Institute for Materials Science, Tsukuba 305-0044, Japan*
[2]*Major of Semiconductor Physics, Korea Maritime University, Pusan 606-791, Republic of Korea*
[3]*Doctoral Program in Materials Science and Engineering, Graduate School of Pure and Applied Sciences, University of Tsukuba, Tsukuba 305-0044, Japan*

(Received 20 November 2008; accepted 24 February 2009; published online 16 March 2009)

Dislocation-related luminescence from small-angle grain boundaries (SA-GBs) in multicrystalline Si was investigated by cathodoluminescence. D3 and D4 emissions were detected at SA-GBs with a misorientation angle of around 1°–1.5°, and D1 and D2 at SA-GBs with a misorientation angle of around 2°–2.5°. Electron beam-induced current investigations indicate that the former SA-GBs possess only shallow energy levels, while the latter possess both deep and shallow levels. The origins of D-line luminescence at SA-GBs are discussed in terms of dislocation structures. © *2009 American Institute of Physics*. [DOI: 10.1063/1.3099001]

The control of grain boundaries (GBs) is the key to improving the efficiency of multicrystalline silicon (mc-Si) solar cells. Previous studies suggest that GBs are carrier recombination centers with shallow and/or deep levels. The GB structure and impurity contamination are likely to affect this recombination strength of GBs.[1–6] We have recently contributed some results to the ongoing discussion on the recombination activities of GBs. The recombination activity of various GBs in high purity mc-Si samples were characterized by the electron-beam-induced current (EBIC) technique.[7,8] We have found that the large-angle GBs (such as Σ and random) were electrically inactive at room temperature but became active when decorated with impurities such as Fe. Similar results for other transition metal impurity attachments have also been presented.[9]

On the other hand, the electrical activity of small-angle (SA)-GBs was rather complicated.[10,11] At room temperature, most SA-GBs did not show obvious EBIC contrast, whereas some SA-GBs did, suggesting they were electrically active. At low temperatures such as 100 K, however, all the SA-GBs showed strong EBIC contrast. It is difficult to explain these phenomena from EBIC observations alone.

It is well known that SA-GBs are composed of dislocation arrays. Since dislocations in bulk Si crystals show characteristic luminescence, named D-lines,[12] it is anticipated that SA-GBs may also yield D-lines. Looking back at D-lines, Drozdov *et al.*[12] have found dislocation luminescence in deformed Si. The luminescence lines at 0.812, 0.875, 0.934, and 1.000 eV were labeled as D1, D2, D3 and D4, respectively. Extensive studies on D-lines were subsequently carried out in Si (Refs. 13–16) and SiGe/Si.[17–21] The nature of the D3 and D4 lines is generally thought to be related to electronic transitions within dislocation cores.[22] However, the origins of D1 and D2 are less clear. It has been argued that they originate in electronic transitions at the geometrical kinks on dislocations,[13] point defects,[14] and impurities[17] in the strain field around dislocations, and/or from the reaction products of dislocations.[15]

In this paper, we tried to clarify the electrical and optical properties of SA-GBs by a combination of EBIC and cathodoluminescence (CL) investigations. High purity mc-Si ingots grown using multistage solidification control were used in this study.[23] Semiconductor-grade Si feedstock was used to reduce the residual impurities. The dopant impurity was *B* at a concentration of 10^{16} cm^{-3}. Atomic absorption spectrophotometry revealed that most metallic impurities, except Fe, were below the detection limit. The Fe concentration was less than 5×10^{12} cm^{-3} at the center of the ingot and in the order of 10^{15}–10^{16} cm^{-3} at the bottom and top of the ingot. To avoid the effects of Fe contamination, we used mc-Si wafers cut from the central part.

For EBIC observations, samples were mechanically rubbed with carborundum and chemically polished with CP4 solution. Schottky contacts with a thickness of 25 nm were prepared by Al deposition. EBIC measurements were carried out using a Hitachi S4200 field-emission scanning electron microscope (FE-SEM) in EBIC mode at both 300 and 100 K.[24] The electron beam energy and current for EBIC observations were 20 kV and 2 nA, respectively. The EBIC contrast, which represents the electrical activity of the defect, is defined by

$$C_{\mathrm{EBIC}} = (I_0 - I_{\mathrm{GB}})/I_0,$$

where I_0 and I_{GB} are the EBIC currents in the background region and at the GB, respectively. After EBIC measurement, the Al Schottky layer was chemically etched off, and the GB character was analyzed by electron backscattered diffraction (EBSD). Subgrain boundaries with a misorientation angle of less than 15° were regarded as SA-GBs. The samples were then characterized by the CL system installed in a Hitachi S4200 FE-SEM at 20 K. The electron beam energy and current for CL observation were 20 kV and 16 nA, respectively. Infrared (IR) emission was detected using an IR-CL system composed of a monochromator and IR-photomultiplier. The D-lines, namely, D1 (0.812 eV), D2 (0.875 eV), D3 (0.934 eV), and D4 (1.00 eV), were observed as in CL spectra and

a)Author to whom correspondence should be addressed. Tel.: 81-29-860-4297. FAX: 81-29-860-4794. Electronic mail: sekiguchi.takashi@nims.go.jp.

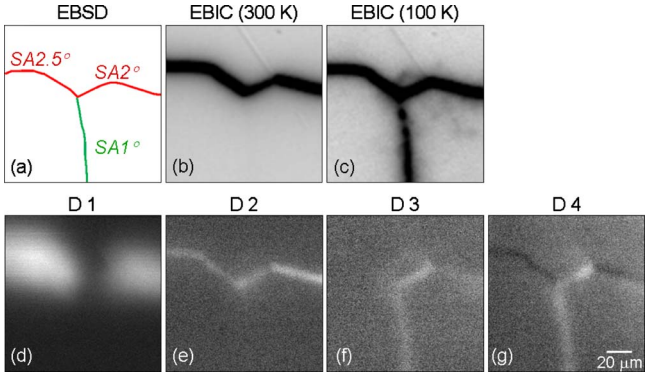

FIG. 1. (Color online) EBSD (a), EBIC [(b) and (c)], and corresponding monochromatic CL [(d)–(g)] images of SA-GBs in mc-Si. The EBIC images were taken at 300 and 100 K. The monochromatic CL images were taken at 0.812 eV (1530 nm), 0.875 eV (1425 nm), 0.934 eV (1333 nm), and 1.000 eV (1240 nm) at 20 K.

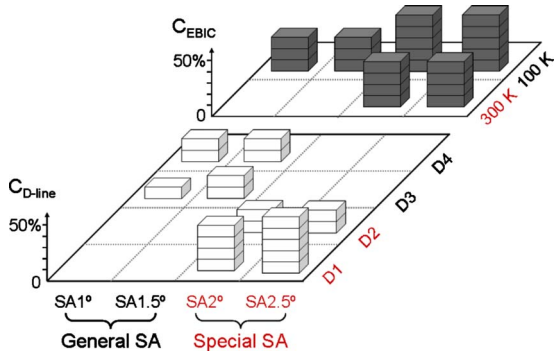

FIG. 2. (Color online) Classification of the contrasts of EBIC and D-lines with respect to the misorientation angle of SA-GBs. The general SA-GBs (1°–1.5°) give the lines D3 and D4, with no obvious EBIC contrast at 300 K, while the special SA-GBs (2°–2.5°) give the lines D1 and D2, with strong EBIC contrast at 300 K.

the corresponding monochromatic CL images. We define the contrast of D-line luminescence by

$$C_{\text{D-line}} = (DL_{\text{GB}} - DL_0)/DL_0,$$

where DL_{GB} and DL_0 are the intensities of D-line luminescence at GBs and the background, respectively. Finally, some of the characterized samples were prepared for transmission electron microscope (TEM) observation at 200 kV.

Figure 1 shows the EBSD, EBIC, and CL images in an mc-Si sample in which three SA-GBs are present. These SA-GBs are represented in the EBSD image by line drawings with their misorientation angles. The SA-GB with a misorientation angle of less than 1° was labeled SA1°. At 300 K, SA1° showed no obvious EBIC contrast, while SA2° and SA2.5° showed strong EBIC contrast, and at 100 K, they all showed strong EBIC contrast. According to the monochromatic CL images, D1 and D2 emissions were chiefly detected at or near the SA2° and the SA2.5°, while D3 and D4 emissions were chiefly detected at the SA1° and part of the SA2°. It should be noted that the D1 emissions were considerably more blurred than the other D-lines. CL spectra (not shown here) also revealed weak peaks at each D-line position, as well as an intense transverse optical phonon replica peak at 1.1 eV (inherent in Si crystal). Due to the weak nature of these signals, it is not possible to discuss the detailed profiles of the D-lines. We also performed these experiments on other samples with different SA-GBs, and found SA1.5° to behave quite similarly to SA1°. No D-lines were observed from large-angle GBs.

Figure 2 shows the relation of EBIC and CL contrasts with respect to the misorientation angle of SA-GBs. Based on the EBIC contrast at 300 K, we divided these SA-GBs into two groups, namely, "general" and "special" SA-GBs. The former show no obvious EBIC contrast, while the latter show significant EBIC contrast. Correspondingly, it is clearly seen that the general SA-GBs have D3 and D4 emissions, while the special ones show D1 and D2 emissions.

Figure 3 shows the TEM images of boundary dislocations of SA1° and SA2.5°. The SA1° was composed of an array of individual edge dislocations with an interval of around 60 nm. The SA2.5° was composed of parallel dislocations with an average spacing of less than 10 nm. These images closely correspond with the dislocation model for SA-GBs.[25]

Based on our EBIC/CL observations, we now discuss the origin of the electrical and optical activities of SA-GBs. General SA-GBs, such as SA1° and SA1.5°, possess only shallow levels and show D3 and D4 lines. These properties can be attributed to individual dislocations. Straight-glide dislocations without metallic contamination are already proved to show D3 and D4 lines.[15] The special SA-GBs, such as SA2° and SA2.5°, possess both deep and shallow levels and show D1 and D2 lines. In this study, the misorientation angle of the special SA-GBs was around 2°, indicating them to be composed of edge dislocations with smaller intervals such as 10 nm. Thus, the energy levels of dislocations may overlap with each other or be affected by the strain field of adjacent dislocations. We therefore conclude that these interactions are what yield the deep energy levels and D1 and D2 emissions. Drozdov *et al.*[12] have reported that D1 and D2 are dominant in heavily deformed Si crystals, while D3 and D4 predominate in weakly deformed Si. Our CL results for SA-GBs are similar to those in the report of Drozdov *et al.*[12] on deformed Si crystals.

It has been pointed out that only the D1 emissions were widely blurred around SA. Although it is still difficult to identify the origin of D1 emissions, this blurred CL image suggests that the carrier recombination mechanism of D1 is different from those of other *D*-lines. Since this hypothesis has not been fully examined, no settled conclusion has been reached.

In summary, the dislocation-related luminescence at SA-GBs in mc-Si was observed by monochromatic CL imaging of D-lines. The general SA-GBs of 1°–1.5° show the D3 and D4 lines, while the special SA-GBs of 2°–2.5° show D1 and D2 lines. Comparing the EBIC data shows these D-lines to be correlated with shallow levels in the former case but with both deep and shallow levels in the latter.

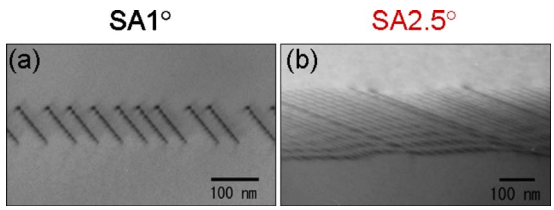

FIG. 3. (Color online) TEM images of boundary dislocations at a general SA1° (a) and a special SA2.5° (b) in high purity mc-Si.

W.L. would like to express his gratitude for the support provided by The Korea Research Foundation Grant (Grant No. KRF-2007-612-C00042), funded by the Korean government.

[1]K. Yang, G. H. Schwuttke, and T. F. Ciszek, J. Cryst. Growth **50**, 301 (1980).
[2]A. Bary and G. Nouet, J. Appl. Phys. **63**, 435 (1988).
[3]J. L. Maurice and C. Colliex, Appl. Phys. Lett. **55**, 241 (1989).
[4]R. Rizk, A. Ihlal, and X. Portier, J. Appl. Phys. **77**, 1875 (1995).
[5]M. Kittler, W. Seifert, M. Stemmer, and J. Palm, J. Appl. Phys. **77**, 3725 (1995).
[6]Z. J. Wang, S. Tsurekawa, K. Ikeda, T. Sekiguchi, and T. Watanabe, Interface Sci. **7**, 197 (1999).
[7]J. Chen, T. Sekiguchi, D. Yang, F. Yin, K. Kido, and S. Tsurekawa, J. Appl. Phys. **96**, 5490 (2004).
[8]J. Chen, D. Yang, Z. Xi, and T. Sekiguchi, J. Appl. Phys. **97**, 033701 (2005).
[9]T. Buonassisi, A. A. Istratov, M. D. Pickett, M. A. Marcus, T. F. Ciszek, and E. R. Weber, Appl. Phys. Lett. **89**, 042102 (2006).
[10]J. Chen, T. Sekiguchi, R. Xie, P. Ahmet, T. Chikyo, D. Yang, S. Ito, and F. Yin, Scr. Mater. **52**, 1211 (2005).
[11]J. Chen and T. Sekiguchi, Jpn. J. Appl. Phys., Part 1 **46**, 6489 (2007).
[12]N. A. Drozdov, A. A. Patrin, and V. D. Tkachev, Zh. Eksp. Teor. Fiz. Pis'ma Red. **23**, 651 (1976); Sov. Phys. JETP **23**, 597 (1976).
[13]M. Suezawa and K. Sumino, Phys. Status Solidi A **78**, 639 (1983).
[14]R. Sauer, J. Weber, J. Stolz, E. R. Weber, K.-H. Küsters, and H. Alexander, Appl. Phys. A: Solids Surf. **36**, 1 (1985).
[15]T. Sekiguchi and K. Sumino, J. Appl. Phys. **79**, 3253 (1996).
[16]M. Kittler, W. Seifert, T. Arguirov, I. Tarasov, and S. Ostapenko, Sol. Energy Mater. Sol. Cells **72**, 465 (2002).
[17]V. Higgs, P. Kightley, P. J. Goodhew, and P. D. Augustus, Appl. Phys. Lett. **59**, 829 (1991).
[18]V. Higgs, E. C. Lightowler, S. Tajbakhsh, and P. J. Wright, Appl. Phys. Lett. **61**, 1087 (1992).
[19]M. Kittler, W. Seifert, and V. Higgs, Phys. Status Solidi A **137**, 327 (1993).
[20]M. Kittler, C. Ulhaq-Bouillet, and V. Higgs, Mater. Sci. Eng., B **24**, 52 (1994).
[21]T. Sumitomo, H. Kita, and S. Matsumoto, Mater. Sci. Semicond. Process. **9**, 794 (2006).
[22]V. V. Kveder, E. A. Steinman, S. A. Shevchenko, and H. G. Grimmeiss, Phys. Rev. B **51**, 10520 (1995).
[23]S. Nara, T. Sekiguchi, and J. Chen, Eur. Phys. J.: Appl. Phys. **27**, 389 (2004).
[24]T. Sekiguchi and K. Sumino, Rev. Sci. Instrum. **66**, 4277 (1995).
[25]W. T. Read and W. Shockley, Phys. Rev. **78**, 275 (1950).